

**CHIRAL SYMMETRY AND THE NUCLEON-NUCLEON
INTERACTION:
DEVELOPING AN ACCURATE NN POTENTIAL BASED
UPON CHIRAL EFFECTIVE FIELD THEORY ***

D. R. ENTEM[†] AND R. MACHLEIDT

*Department of Physics, University of Idaho, Moscow, ID 83844, USA
E-mails: dentem@uidaho.edu, machleid@uidaho.edu*

We present an accurate nucleon-nucleon (NN) potential based upon chiral effective Lagrangians. The model includes one- and two-pion exchange contributions up to chiral order three and contact terms (which represent the short range force) up to order four. Within this framework, the NN phase shifts below 300 MeV lab. energy and the properties of the deuteron are reproduced with high-precision. This chiral NN potential may serve as a reliable starting point for testing the chiral effective field theory approach in exact few-nucleon and microscopic nuclear many-body calculations.

1 Introduction

One of the most fundamental problems of nuclear physics is to derive the force between two nucleons from first principles. A great obstacle for the solution of this problem has been the fact that the fundamental theory of strong interaction, QCD, is nonperturbative in the low-energy regime characteristic for nuclear physics. The way out of this dilemma is the effective field theory concept which recognizes different energy scales in nature. Below the chiral symmetry breaking scale, $\Lambda_\chi \approx 1$ GeV, the appropriate degrees of freedom are pions and nucleons interacting via a force that is governed by the symmetries of QCD, particularly, (broken) chiral symmetry.

The derivation of the nuclear force from chiral effective field theory was pioneered by Weinberg¹, Ordóñez,² and van Kolck.^{3,4} Important contributions were made by Robilotta *et al.*,⁵ Kaiser *et al.*,^{6,7,8} and Epelbaum *et al.*⁹ As a result, efficient methods for deriving the nuclear force from chiral Lagrangians have emerged. Also, the quantitative nature of the chiral NN potential has improved.⁹ Nevertheless, even the currently ‘best’ chiral NN potentials are too inaccurate to serve as a reliable input for exact few-nucleon calculations or microscopic nuclear many-body theory.

*INVITED TALK PRESENTED AT THE 7-TH INTERNATIONAL SPRING SEMINAR ON NUCLEAR STRUCTURE PHYSICS “CHALLENGES OF NUCLEAR STRUCTURE”, MAIORI (NEAR NAPLES, ITALY) MAY 27-31, 2001.

[†]ON LEAVE FROM UNIVERSITY OF SALAMANCA, SPAIN.

The time has come to put the chiral approach to a real test in microscopic nuclear structure physics. Conclusive results can, however, be produced only with a 100% quantitative NN potential based upon chiral Lagrangians. For this reason, we have embarked on a program to develop a NN potential that is based upon chiral effective field theory and reproduces the NN data with about that same quality as the high-precision NN potentials constructed in the 1990's.^{10,11,12}

In Secs. 2 to 5, we will develop, step by step, the chiral NN potential; and in Sec. 6 we will show that we have achieved our goal.

2 Effective Chiral Lagrangian

The effective chiral πN Lagrangian is given by a series of terms of increasing chiral dimension,¹³

$$\mathcal{L}_{\pi N} = \mathcal{L}_{\pi N}^{(1)} + \mathcal{L}_{\pi N}^{(2)} + \mathcal{L}_{\pi N}^{(3)} + \dots, \quad (1)$$

where the superscript refers to the number of derivatives or pion masses (chiral dimension) and the ellipsis denotes terms of chiral order four or higher.

At lowest order, the Lagrangian in its relativistic form reads

$$\mathcal{L}_{\pi N}^{(1)} = \bar{\Psi} \left(i\gamma^\mu D_\mu - M_N + \frac{g_A}{2} \gamma^\mu \gamma_5 u_\mu \right) \Psi \quad (2)$$

with

$$D_\mu = \partial_\mu + \Gamma_\mu \quad (3)$$

$$\Gamma_\mu = \frac{1}{2} (\xi^\dagger \partial_\mu \xi + \xi \partial_\mu \xi^\dagger) \approx \frac{i}{4f_\pi^2} \boldsymbol{\tau} \cdot (\boldsymbol{\pi} \times \partial_\mu \boldsymbol{\pi}) + \dots \quad (4)$$

$$u_\mu = i(\xi^\dagger \partial_\mu \xi - \xi \partial_\mu \xi^\dagger) \approx -\frac{1}{f_\pi} \boldsymbol{\tau} \cdot \partial_\mu \boldsymbol{\pi} + \dots \quad (5)$$

$$U = \xi \xi \quad (6)$$

$$\xi = e^{i\boldsymbol{\tau} \cdot \boldsymbol{\pi} / 2f_\pi} \approx 1 + \frac{i\boldsymbol{\tau} \cdot \boldsymbol{\pi}}{2f_\pi} - \frac{\boldsymbol{\pi}^2}{8f_\pi^2} + \dots \quad (7)$$

For the parameters that occur in the first order Lagrangian, we use $M_N = 938.9187$ MeV, $f_\pi = 92.4$ MeV, and $g_A = g_{\pi NN} f_\pi / M_N = 1.29$; the latter is equivalent to $g_{\pi NN}^2 / 4\pi = 13.67$.

We will apply the heavy baryon (HB) formulation of chiral perturbation theory¹⁴ in which the relativistic Lagrangian is subjected to an expansion in terms of powers of $1/M_N$ (kind of a nonrelativistic expansion), the lowest

order of which is

$$\widehat{\mathcal{L}}_{\pi N}^{(1)} = \bar{N} \left(iD_0 - \frac{g_A}{2} \vec{\sigma} \cdot \vec{u} \right) N \quad (8)$$

$$\approx \bar{N} \left[i\partial_0 - \frac{1}{4f_\pi^2} \boldsymbol{\tau} \cdot (\boldsymbol{\pi} \times \partial_0 \boldsymbol{\pi}) - \frac{g_A}{2f_\pi} \boldsymbol{\tau} \cdot (\vec{\sigma} \cdot \vec{\nabla}) \boldsymbol{\pi} \right] N + \dots \quad (9)$$

In the relativistic formulation, the field operators representing nucleons, Ψ , contain four-component Dirac spinors; while in the HB version, the field operators, N , contain Pauli spinors; in addition, all nucleon field operators contain Pauli spinors describing the isospin of the nucleon.

At second order, the relativistic Lagrangian reads

$$\mathcal{L}_{\pi N}^{(2)} = \sum_{i=1}^4 c_i \bar{\Psi} O_i^{(2)} \Psi. \quad (10)$$

The various operators $O_i^{(2)}$ are given in Ref.¹³. The fundamental rule by which this Lagrangian—as well as all the other ones—are assembled is that they must contain *all* terms consistent with chiral symmetry and Lorentz invariance (apart from the other trivial symmetries) at a given chiral dimension (here: order two). The parameters c_i are known as low-energy constants (LECs) and must be determined empirically from fits to πN data. We use the values determined by Büttiker and Meißner,¹⁵ which are (in units of GeV^{-1}),

$$c_1 = -0.81, \quad c_3 = -4.70, \quad c_4 = 3.40; \quad (11)$$

c_2 will not be needed.

The HB projected Lagrangian at order two is most conveniently broken up into two pieces,

$$\widehat{\mathcal{L}}_{\pi N}^{(2)} = \widehat{\mathcal{L}}_{\pi N, \text{fix}}^{(2)} + \widehat{\mathcal{L}}_{\pi N, \text{ct}}^{(2)}, \quad (12)$$

with

$$\widehat{\mathcal{L}}_{\pi N, \text{fix}}^{(2)} = \bar{N} \left[\frac{1}{2M_N} \vec{D} \cdot \vec{D} + i \frac{g_A}{4M_N} \{ \vec{\sigma} \cdot \vec{D}, u_0 \} \right] N \quad (13)$$

and

$$\begin{aligned} \widehat{\mathcal{L}}_{\pi N, \text{ct}}^{(2)} = \bar{N} & \left[2c_1 m_\pi^2 (U + U^\dagger) + \left(c_2 - \frac{g_A^2}{8M_N} \right) u_0^2 + c_3 u_\mu u^\mu \right. \\ & \left. + \frac{i}{2} \left(c_4 + \frac{1}{4M_N} \right) \vec{\sigma} \cdot (\vec{u} \times \vec{u}) \right] N. \end{aligned} \quad (14)$$

Note that $\widehat{\mathcal{L}}_{\pi N, \text{fix}}^{(2)}$ is created entirely from the HB expansion of the relativistic $\mathcal{L}_{\pi N}^{(1)}$ and thus has no free parameters (“fixed”), while $\widehat{\mathcal{L}}_{\pi N, \text{ct}}^{(2)}$ is dominated by

the new πN contact terms proportional to the c_i parameters, besides some small $1/M_N$ corrections.

At third order, the relativistic Lagrangian can be formally written as

$$\mathcal{L}_{\pi N}^{(3)} = \sum_{i=1}^{23} d_i \bar{\Psi} O_i^{(3)} \Psi, \quad (15)$$

with the operators, $O_i^{(3)}$, listed in Refs.^{13,16}; not all 23 terms are relevant to our problem. Similar to the order two case, the HB projected Lagrangian at order three is,

$$\widehat{\mathcal{L}}_{\pi N}^{(3)} = \widehat{\mathcal{L}}_{\pi N, \text{fix}}^{(3)} + \widehat{\mathcal{L}}_{\pi N, \text{ct}}^{(3)}, \quad (16)$$

with

$$\begin{aligned} \widehat{\mathcal{L}}_{\pi N, \text{fix}}^{(3)} = & + \frac{g_A}{8M_N^2} \bar{N} \overleftarrow{D} \cdot (\vec{\sigma} \cdot \vec{u}) \vec{D} N \\ & - \frac{g_A}{8M_N^2} \bar{N} \left[(\vec{\sigma} \cdot \overleftarrow{D}) (\vec{u} \cdot \vec{D}) + \text{h.c.} \right] N \\ & + \frac{g_A}{16M_N^2} \bar{N} \left[(\vec{\sigma} \cdot \vec{u}) \vec{D}^2 + \text{h.c.} \right] N + \dots, \end{aligned} \quad (17)$$

the ellipsis standing for relativistic correction terms not needed here, and $\widehat{\mathcal{L}}_{\pi N, \text{ct}}^{(3)}$ given in Refs.^{13,16}; the latter reference contains also a determination of the d_i LECs.

3 Pion-Exchange Diagrams and Power Counting

The πN Lagrangian constructed in the previous section is the crucial ingredient for the evaluation of the pion-exchange contributions to the NN interaction. Since we are dealing here with a low-energy effective theory, it is appropriate to analyze the contributions in terms of powers of small momenta: $(Q/\Lambda_\chi)^\nu$, where Q is a generic momentum or a pion mass and $\Lambda_\chi \approx 1$ GeV is the chiral symmetry breaking scale. This procedure has become known as *Power Counting*. For the pion-exchange diagrams relevant to our problem, the power ν of a diagram is determined by the simple formula

$$\nu = 2 \times \text{loops} + \sum_j (d_j - 1), \quad (18)$$

where ‘loops’ denotes the number of loops in the diagram, d_j the number of derivatives involved in vertex j , and the sum runs over all vertices.

The most important irreducible one-pion exchange (OPE) and two-pion exchange (TPE) contributions to the NN interaction up to order Q^3 are shown

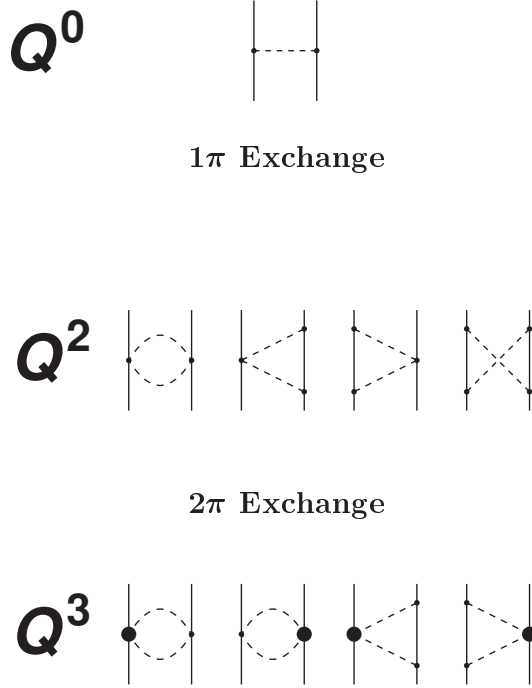


Figure 1. The most important irreducible one- and two-pion exchange contributions to the NN interaction up to order Q^3 . Vertices denoted by small dots are from $\widehat{\mathcal{L}}_{\pi N}^{(1)}$, while large dots refer to $\widehat{\mathcal{L}}_{\pi N, \text{ct}}^{(2)}$.

in Fig. 1; they have been evaluated by Kaiser *et al.*⁶ using covariant perturbation theory and dimensional regularization. In addition to the diagrams displayed, we take into account the relativistic corrections up to order three as implied by $\widehat{\mathcal{L}}_{\pi N, \text{fix}}^{(2)}$, Eq. (13) and $\widehat{\mathcal{L}}_{\pi N, \text{fix}}^{(3)}$, Eq. (17), where the latter contributes only to the one-pion exchange—to the order we are working at.

One- and two-pion exchanges are known to describe NN scattering in peripheral partial waves. Therefore, we show in Fig. 2 (solid line) predictions by the chiral model displayed in Fig. 1 (plus relativistic corrections up to order three) for the phase shifts in G waves. To provide a comparison with conventional meson theory, we show also the predictions for $\pi + 2\pi$ exchange by the Bonn model¹⁷ (dashed line). The dotted line represents pure one-pion exchange. Note that our calculations with 2π models always include also the

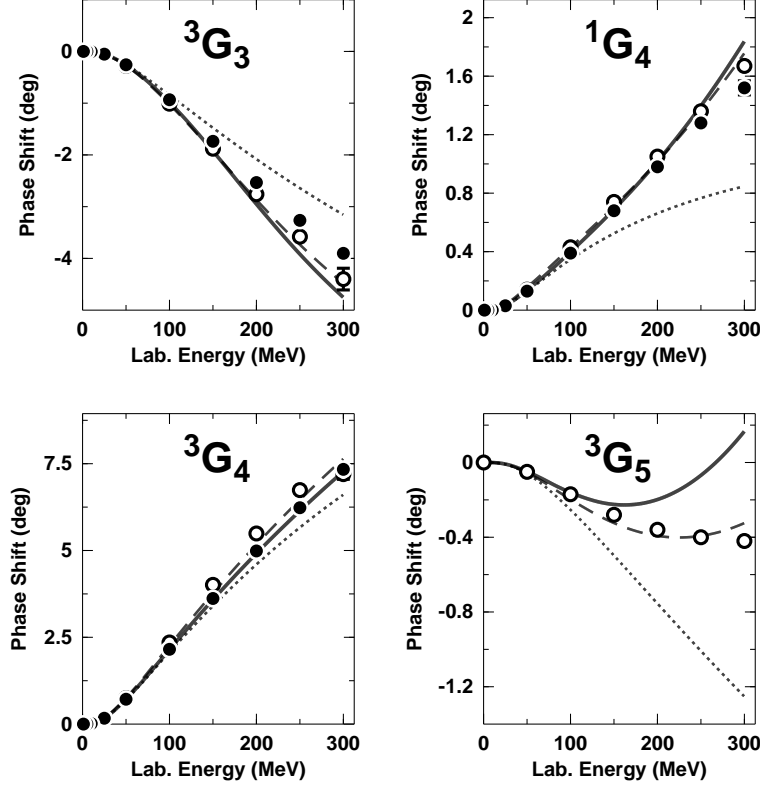


Figure 2. G -wave phase shifts. The predictions from the chiral model displayed in Fig. 1 are shown by the solid curve and the ones from the Bonn model¹⁷ by the dashed curve. The dotted curve is OPE. Solid dots represent the Nijmegen multi-energy np analysis¹⁸ and open circles the VPI/GWU analysis.¹⁹

iterated one-pion exchange. From Fig. 2 we can conclude that, in G waves (orbital angular momentum $L = 4$), there is good agreement between the chiral and conventional 2π model as well as the empirical phase shifts. This is also true for all partial waves with $L > 4$.

The agreement deteriorates when proceeding to lower L . While in F waves the agreement between the chiral model and the empirical phase shifts is still fair, substantial discrepancies emerge in D waves as demonstrated in Fig. 3: the chiral 2π exchange is far too attractive—a fact that has been

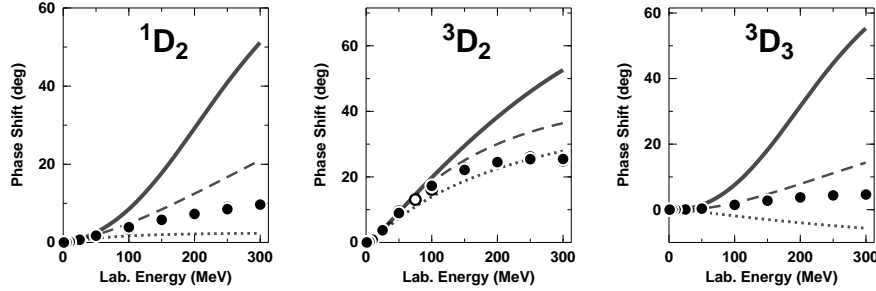


Figure 3. D -wave phase shifts. Notation as in Fig. 2.

noticed before.^{6,7}

4 Short-Range/Contact Contributions

To control the D (and lower) partial waves, we need (repulsive) short-range contributions. In the conventional meson model, these are created by the exchange of heavy mesons (notably, the ω meson). In chiral perturbation theory (χ PT), heavy mesons have no place and the short-range force is parametrized in terms of contact potentials, which are organized by powers of Q . If Q is, e. g., a momentum transfer, i. e., $\vec{Q} = \vec{p}' - \vec{p}$, where \vec{p} and \vec{p}' are the CM nucleon momenta before and after scattering, respectively, and θ is the scattering angle, then, for even ν ,

$$\vec{Q}^\nu \sim (\cos \theta)^m \quad \text{with} \quad m \leq \frac{\nu}{2}. \quad (19)$$

Partial-wave decomposition for orbital-angular momentum L yields,

$$\int_{-1}^{+1} \vec{Q}^\nu P_L(\cos \theta) d \cos \theta \neq 0 \quad \text{for} \quad L \leq \frac{\nu}{2}, \quad (20)$$

where P_L is a Legendre polynomial. The conclusion is that for non-vanishing contributions in D waves ($L = 2$), $\nu = 4$ is required. Based upon invariance considerations, there are a total of 24 contact terms up to order Q^4 , which we all include in our model. The parameters of these terms have to be natural, but are otherwise not restricted and, thus, represent essentially free parameters.

The ideas of χ PT may suggest that, if contacts are included up to order four, then also the 2π contribution should be calculated up to order four. (We went up to third order in the previous section, cf. Fig. 1.) We have looked

into this issue and found that the current status of the chiral 2π exchange at order four is a Pandora's Box. Some contributions have been calculated, like the football diagram with both vertices taken from $\widehat{\mathcal{L}}_{\pi N, ct}^{(2)}$, i. e., both vertices proportional to one of the LECs c_i . It turns out²⁰ that the attraction generated by this diagram alone is so huge that it essentially doubles the size of the chiral 2π exchange in peripheral partial waves, leading to very serious (irreparable?) discrepancies with the empirical phase shifts and the predictions by conventional meson-exchange models. Other contributions at order four are obtained by inserting for the solid-dot vertices in Fig. 1 interactions from $\widehat{\mathcal{L}}_{\pi N, ct}^{(3)}$ (proportional to the LECs d_i). Consistency requires that these diagrams are calculated together with corresponding two-loop contributions of order four. All this is very involved and it will create horrific mathematical expression to just describe the long-range NN interaction. At this time, nothing is known about these contributions, but the most optimistic prognosis would be that the latter contributions will compensate the enormous attraction from the c_i^2 football. But even if this optimistic scenario were to come true, the chiral model would no longer be practical for nuclear physics purposes. It may then be much more reasonable to use the 'resonance saturation' argument and return to the conventional meson models of the past, particularly, the beautiful and simple one-boson-exchange model:²¹ in this model the one-sigma exchange (the mathematical expression for which can be written in just one line) describes the entire 2π exchange—quantitatively!

In conclusion: for the time being, the only realistic avenue towards a quantitative NN potential based upon χ PT is a 'split approach': chiral 2π up to order three, contacts up to order four. This is our model.

5 The NN Potential

Since the 2π exchange diagrams, Fig. 1, are calculated using covariant perturbation theory,⁶ it is appropriate to start from the Bethe-Salpeter (BS) equation²² which reads in operator notation

$$\mathcal{T} = \mathcal{V} + \mathcal{V} \mathcal{G} \mathcal{T} \quad (21)$$

with \mathcal{T} the invariant amplitude for the two-nucleon scattering process, \mathcal{V} the sum of all connected two-particle irreducible diagrams, and \mathcal{G} the relativistic two-nucleon propagator. The BS equation is equivalent to a set of two equations:

$$\mathcal{T} = \bar{V} + \bar{V} g \mathcal{T} \quad (22)$$

$$\bar{V} = \mathcal{V} + \mathcal{V} (\mathcal{G} - g) \bar{V} \quad (23)$$

$$\approx \mathcal{V} + \mathcal{V}_{\text{OPE}} (\mathcal{G} - g) \mathcal{V}_{\text{OPE}} \quad (24)$$

where the last line states the approximation we are using, exhibiting the way we treat the 2π box diagram (\mathcal{V}_{OPE} is the relativistic one-pion exchange and \mathcal{V} contains all the irreducible diagrams of the type displayed in Fig. 1, including relativistic corrections up to order three). This treatment avoids double counting when \bar{V} is iterated in the scattering equation and is also consistent with the calculations of Ref.⁶. For the relativistic three-dimensional propagator g , we choose the one proposed by Blankenbecler and Sugar²³ (BbS)^a which has the great practical advantage that the OPE (and the entire potential) becomes energy-independent. Thus, we do not need the rather elaborate formalism of unitary transformations⁹ to generate energy-independence of the potential.

Our full chiral NN potential \bar{V} is defined by

$$\bar{V}(\vec{p}', \vec{p}) \equiv \left\{ \begin{array}{l} \text{sum of irreducible} \\ \pi + 2\pi \text{ contributions} \end{array} \right\} + \text{contacts}, \quad (25)$$

where the first term on the r.h.s. is given by Eq. (24).

This potential satisfies the relativistic BbS equation, Eq. (22). If we define now,

$$V(\vec{p}', \vec{p}) \equiv \sqrt{\frac{M_N}{E_{p'}}} \bar{V}(\vec{p}', \vec{p}) \sqrt{\frac{M_N}{E_p}} \approx \left(1 - \frac{p'^2 + p^2}{4M_N^2} \right) \bar{V}(\vec{p}', \vec{p}) \quad (26)$$

with $E_p \equiv \sqrt{M_N^2 + p^2}$, then V satisfies the usual, nonrelativistic Lippmann-Schwinger (LS) equation,

$$T(\vec{p}', \vec{p}) = V(\vec{p}', \vec{p}) + \int d^3p'' V(\vec{p}', \vec{p}'') \frac{M}{p^2 - p''^2 + i\epsilon} T(\vec{p}'', \vec{p}). \quad (27)$$

Note that the correction term $-(p'^2 + p^2)/4M_N^2$ in Eq. (26) is included only for OPE; for TPE it would create contributions beyond the order to which we calculate and for contacts it creates either existing terms or goes beyond our accuracy.

In summary, our chiral NN potential V is defined by Eq. (26) with \bar{V} as given in Eq. (25). Since V satisfies Eq. (27), it is suitable for application in conventional, nonrelativistic nuclear structure physics.

Iteration of V in the LS equation requires cutting V off for high momenta to avoid infinities. Therefore, we regularize V in the following way:

$$V(\vec{p}', \vec{p}) \mapsto V(\vec{p}', \vec{p}) e^{-(p'/\Lambda)^{2n}} e^{-(p/\Lambda)^{2n}} \quad (28)$$

^aFor a derivation of the BbS approach, see appendix A.1 of Ref.¹².

$$\approx V(\vec{p}', \vec{p}) \left\{ 1 - \left[\left(\frac{p'}{\Lambda} \right)^{2n} + \left(\frac{p}{\Lambda} \right)^{2n} \right] + \dots \right\}, \quad (29)$$

where the last equation gives an indication of the fact that the exponential cutoff does not affect the order to which we are calculating, but introduces contributions beyond that order. For the contact potentials, we use cutoff masses Λ which are partial wave dependent. One can show that in doing so we just generalize the above regularization concept in the following sense:

$$V(\vec{p}', \vec{p}) \mapsto V(\vec{p}', \vec{p}) \left\{ 1 - b_1 \left[\left(\frac{p'}{\Lambda} \right)^{2n} + \left(\frac{p}{\Lambda} \right)^{2n} \right] + \dots \right\}, \quad (30)$$

with b_i of $\mathcal{O}(1)$.

For OPE, we use $n = 4$ and $\Lambda = 0.6$ GeV; for TPE, $n = 2$ and $\Lambda = 0.46$ GeV; and for the contact potentials, $n = 2$ (except for contacts of order Q^0 where $n = 3$) and $\Lambda \approx 0.4 - 0.5$ GeV. The number of cutoff parameters is 22 which, together with the 24 contact parameters, results in a total of 46 parameters for our model. At first glance, this may sound a lot. Note, however, that the Nijmegen phase shift analysis¹⁸ uses 40 parameters and that the high-precision potentials^{10,11,12} developed in the 1990's have between 40 and 50 parameters. Thus, a precise fit of the NN data requires around 50 parameters, unless a model has more predictive power than the meson model. An important comment that has to be made about the chiral NN potential is that it has very little predictive power—less than the meson model. In the light of this fact, the number of 46 parameters is no surprise.

6 Results for the Two-Nucleon System

6.1 Two-Nucleon Scattering

In Figs. 4 and 5, we show the phase shifts of neutron-proton (np) scattering for lab. energies below 300 MeV and partial waves with $J \leq 2$. The solid line represents the result from the chiral NN potential developed in the present work. *The reproduction of the empirical phase shifts by our model is excellent.* For comparison, we also show the phase shift predictions by two chiral models recently developed by Epelbaum *et al.*⁹ (dotted and dashed curves in Figs. 4 and 5). In the upper part of Table 1, we give our results for the effective range parameters of the S waves which agree accurately with the empirical values. We note that our present chiral potential is charge-independent and adjusted to the np data.

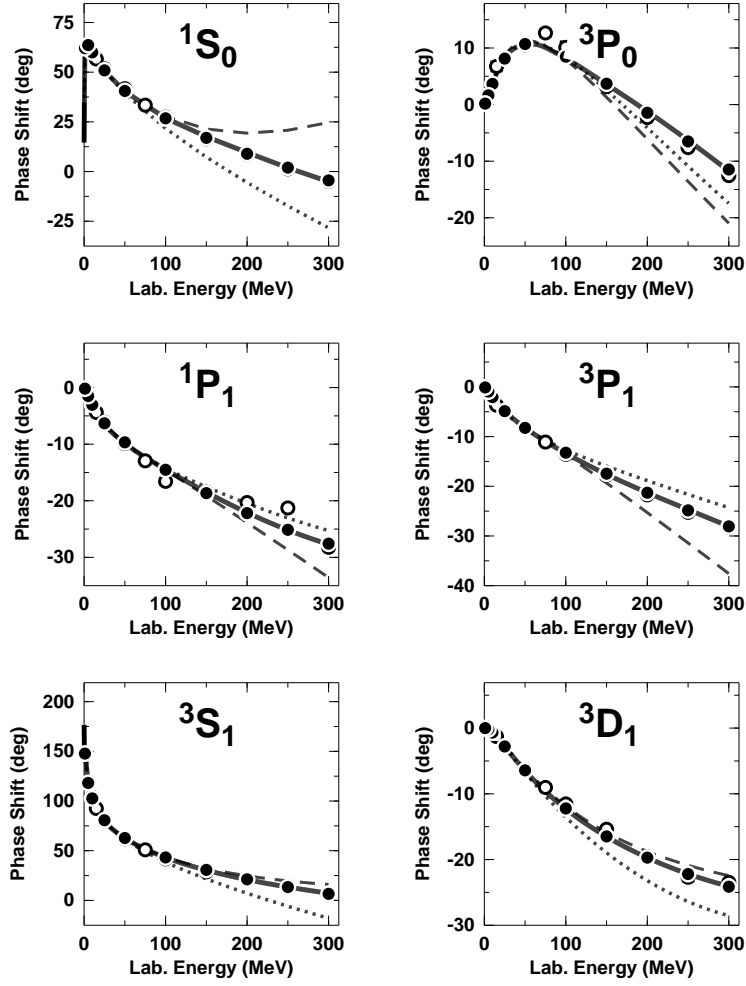


Figure 4. Phase shifts for $J \leq 1$. The solid line is the result from our chiral NN potential, while the dotted and dashed lines are the predictions by two chiral models developed by Epelbaum *et al.* (NLO and NNLO, respectively).⁹ The notation for the empirical points is the same as in Fig. 2.

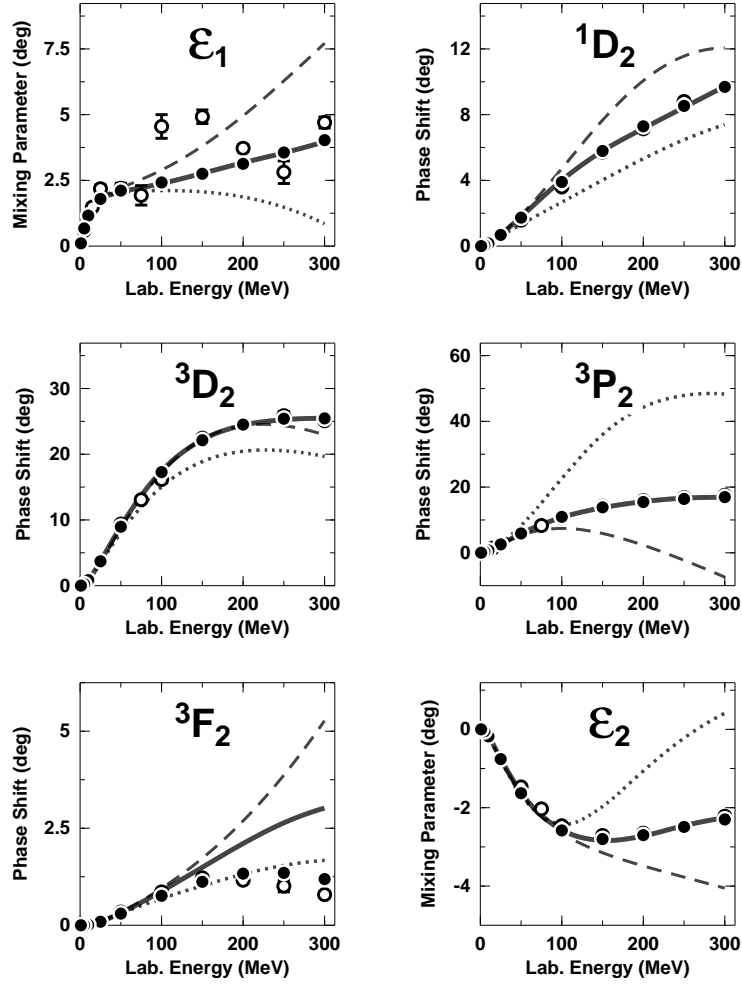


Figure 5. Mixing angle ϵ_1 and $J = 2$ phase parameters. Notation as in Fig. 4.

6.2 The Deuteron

The reproduction of the deuteron parameters is shown in the middle part of Table 1. We present results for two versions of our chiral NN potential,

Table 1. Two- and three-nucleon low-energy data.

	Idaho-A ^a	Idaho-B ^a	CD-Bonn ¹²	AV18 ¹¹	Empirical ^b
Low-energy np scattering					
1S_0 scattering length (fm)	-23.75	-23.75	-23.74	-23.73	-23.74(2)
1S_0 effective range (fm)	2.70	2.70	2.67	2.70	2.77(5)
3S_1 scattering length (fm)	5.417	5.417	5.420	5.419	5.419(7)
3S_1 effective range (fm)	1.750	1.750	1.751	1.753	1.753(8)
Deuteron properties					
Binding energy (MeV)	2.224575	2.224575	2.224575	2.224575	2.224575(9)
Asympt. S state (fm ^{-1/2})	0.8846	0.8846	0.8846	0.8850	0.8846(9)
Asympt. D/S state	0.0256	0.0255	0.0256	0.0250	0.0256(4)
Deuteron radius (fm)	1.9756 ^c	1.9758 ^c	1.970 ^c	1.971 ^c	1.9754(9) ^d
Quadrupole moment (fm ²)	0.281 ^e	0.284 ^e	0.280 ^e	0.280 ^e	0.2859(3)
D -state probability (%)	4.17	4.94	4.85	4.85	5.76
Triton binding (MeV)	8.14	8.02	8.00	7.62	8.48

^aChiral NN potential of the present work.

^bFor references concerning the empirical data, see Tables XIV and XVIII of Ref.¹².

^cWith meson-exchange current (MEC) and relativistic corrections.²⁴

^dReference²⁵.

^eIncluding MEC and relativistic corrections in the amount of 0.010 fm².²⁶

dubbed ‘Idaho-A’ and ‘Idaho-B’.^b The main difference between the two models is in the D -state probability of the deuteron, P_D . Even though P_D is not an observable, it is of theoretical interest since the binding energies of few- and many-nucleon systems depend on it (cf. triton results at the bottom of Table 1). As mentioned before, the predictive power of the chiral model is very limited and it is possible to construct chiral potentials that fit the 3S_1 , 3D_1 , and ϵ_1 phase parameters up to 300 MeV and the empirical deuteron properties accurately, but have D -state probabilities that range from 3 to 6%. Such a large variation of P_D is not possible within the meson model of nuclear forces.

Remarkable are the results produced by our chiral potentials for the deuteron radius which agree accurately with the latest empirical value obtained by using the isotope-shift method.²⁵ All NN potentials of the past (Table 1 includes two representative examples, namely, CD-Bonn¹² and AV18¹¹) fail to reproduce this very precise new value for the deuteron radius.²⁴ Our chiral NN potentials are the first to predict this value right.

In Fig. 6, we display the deuteron wave functions derived from our chiral

^bWe note that the phase shifts represented by the solid line in Figs 4 and 5 are for Idaho-B; however, the ones for Idaho-A are so close to Idaho-B that they could not be distinguished on the scale of the figure.

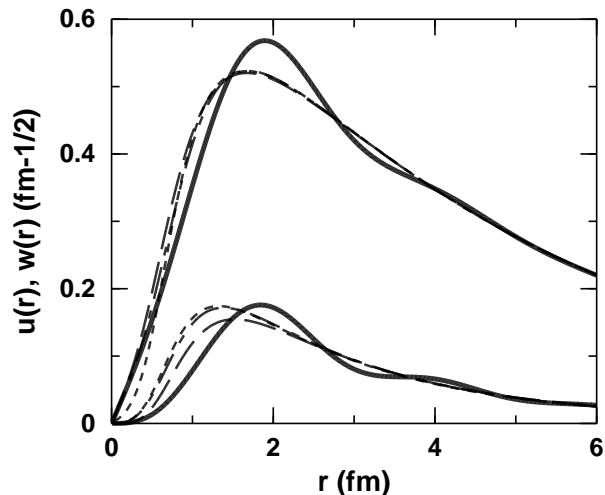


Figure 6. Deuteron wave functions: the larger curves are S -waves, the smaller ones D -waves. The solid line represents the wave functions derived from our chiral NN potential (Idaho-B). The dashed, dash-dotted, and dotted lines refer to the wave functions of the CD-Bonn¹², Nijm-I¹⁰, and AV18¹¹ potentials, respectively.

potential (Idaho-B) by the solid line and compare them with wave functions based upon conventional NN potentials from the recent past. Characteristic differences are noticeable; in particular, the chiral wave functions are shifted towards larger r which explains the larger deuteron radius.

Concerning the triton binding energy predictions given at the bottom of Table 1, we like to comment that the results for Idaho-A and B are obtained in a 34-channel Faddeev calculation with no charge-dependence (i. e., using the np potential throughout), while the corresponding calculations with CD-Bonn and AV18 take charge-dependence into account.

7 Summary and Conclusions

We have constructed an *accurate* chiral NN potential. The model includes one- and two-pion exchange contributions up to chiral order three and contact terms (which represent the short range force) up to order four. Within this framework, the NN phase shifts below 300 MeV lab. energy and the properties of the deuteron are reproduced with high-precision.

Due to the very quantitative nature of this new chiral NN potential, it represents a reliable and promising starting point for exact few-body calculations and microscopic nuclear many-body theory.

Acknowledgments

We gratefully acknowledge useful discussions with B. van Kolck, E. Epelbaum, W. Glöckle, N. Kaiser, U. Meißner, and M. Robilotta. This work was supported in part by the U.S. National Science Foundation under Grant No. PHY-0099444 and by the Ramón Areces Foundation (Spain).

References

1. S. Weinberg, *Phys. Lett. B* **251**, 288 (1990); *Nucl. Phys.* **B363**, 3 (1991).
2. C. Ordóñez and U. van Kolck, *Phys. Lett. B* **291**, 459 (1992).
3. C. Ordóñez, L. Ray, and U. van Kolck, *Phys. Rev. Lett.* **72**, 1982 (1994); *Phys. Rev. C* **53**, 2086 (1996).
4. U. van Kolck, *Prog. Part. Nucl. Phys.* **43**, 337 (1999).
5. C. A. da Rocha and M. R. Robilotta, *Phys. Rev. C* **49**, 1818 (1994); *ibid.* **52**, 531 (1995); J.-L. Ballot *et al.*, *ibid.* **C 57**, 1574 (1998).
6. N. Kaiser, R. Brockmann, and W. Weise, *Nucl. Phys.* **A625**, 758 (1997).
7. N. Kaiser *et al.*, *Nucl. Phys.* **A637**, 395 (1998).
8. N. Kaiser, *Phys. Rev. C* **61**, 014003 (1999); *ibid.* **62**, 024001 (2000); *ibid.* **63**, 044010 (2001).
9. E. Epelbaum, W. Glöckle, and U.-G. Meißner, *Nucl. Phys.* **A637**, 107 (1998); *ibid.* **A671**, 295 (2000).
10. V. G. J. Stoks *et al.*, *Phys. Rev. C* **49**, 2950 (1994).
11. R. B. Wiringa *et al.*, *Phys. Rev. C* **51**, 38 (1995).
12. R. Machleidt, *Phys. Rev. C* **63**, 024001 (2001)
13. N. Fettes, U.-G. Meißner, M. Mojžiš, and S. Steininger, *Ann. Phys. (N.Y.)* **283**, 273 (2000); *ibid.* **288**, 249 (2001).
14. V. Bernard *et al.*, *Int. J. Mod. Phys. E* **4**, 193 (1995).
15. P. Büttiker and U.-G. Meißner, *Nucl. Phys.* **A668**, 97 (2000).
16. N. Fettes *et al.*, *Nucl. Phys.* **A640**, 199 (1998).
17. R. Machleidt, K. Holinde, and Ch. Elster, *Phys. Rep.* **149**, 1 (1987).
18. V. G. J. Stoks *et al.*, *Phys. Rev. C* **48**, 792 (1993).
19. R. A. Arndt *et al.*, SAID, Solution SM99 (Summer 1999).
20. N. Kaiser, private communication.
21. R. Machleidt, *Adv. Nucl. Phys.* **19**, 189 (1989).
22. E. E. Salpeter and H. A. Bethe, *Phys. Rev.* **84**, 1232 (1951).

23. R. Blankenbecler and R. Sugar, *Phys. Rev.* **142**, 1051 (1966).
24. J. L. Friar *et al.*, *Phys. Rev. A* **56**, 4579 (1997).
25. A. Huber *et al.*, *Phys. Rev. Lett.* **80**, 468 (1998).
26. J. Adam and H. Henning, private communication.